

Sugars Electrooxidation at Glassy Carbon Electrode Decorate with Multi-Walled Carbon Nanotubes with Nickel Oxy-Hydroxide

Acelino Cardoso de Sá^{1,*}, Leonardo Lataro Paim², Nelson Ramos Stradiotto¹

¹ Analytical Chemistry Department, Institute of Chemistry, UNESP – Univ Estadual Paulista, 55 Francisco Degni st, 14800-060, Araraquara, SP, Brazil.

² Engineering of Energy, Experimental Campus of Rosana, UNESP – Univ Estadual Paulista, 1881 dos Barrageiros ave, 19274-000, Primavera, Rosana, SP, Brazil.

*E-mail: acelino2@hotmail.com

Received: 30 June 2014 / Accepted: 2 October 2014 / Published: 28 October 2014

The glassy carbon electrode modified with carbon nanotubes decorated with nickel oxy-hydroxide (GC/MWCNT/NiOOH) was used to studied electro-oxidation of glucose, galactose, xylose, arabinose and mannose in alkaline medium. Kinetic parameters such as, charge-transfer coefficient, electrocatalytic rate constant and diffusion coefficient were determined for sugars. Galactose exhibited a higher charge-transfer coefficient (0.37) with a diffusion coefficient of $1.3 \times 10^{-6} \text{ cm}^2 \text{ s}^{-1}$ and showed the higher electrocatalytic rate constant of $2.1 \times 10^4 \text{ L mol}^{-1} \text{ s}^{-1}$. The modified electrode exhibited a linear response to sugars concentration in the range around of $2.5 \times 10^{-4} \text{ mol L}^{-1}$ to $5.6 \times 10^{-3} \text{ mol L}^{-1}$ and limits of detection around of $1.9 \times 10^{-4} \text{ mol L}^{-1}$ - $4.3 \times 10^{-4} \text{ mol L}^{-1}$.

Keywords: Electrocatalytic rate constant of sugars; Kinetic parameters; Nickel oxy-hydroxide; Carbon nanotubes; Chemically modified electrodes.

1. INTRODUCTION

Sugarcane bagasse is a byproduct originated of the process of production of sugar and ethanol. Bagasse is used mainly for generating bioelectricity through burning in boilers into plants of sugarcane. New applications for bagasse have been developed, among which can highlight the production of second-generation biofuels (ethanol) [1]. The great potential of biomass for the production of second generation ethanol is mainly related to the large availability of raw material [1, 2].

The biomass is constituted by three main fractions of lignocellulosic materials, cellulose, hemicellulose and lignin. Cellulose is a homopolysaccharide consisting of a linear chain of $\beta(1 \rightarrow 4)$

linked D-glucose units [3, 4]. Hemicelluloses are a heterogeneous class of polymers containing sugars as pentoses (β -D-xylose, α -L-arabinose), hexoses (β -D-mannose, β -D-glucose, α -D-galactose) and uronic compounds (α -D-glucuronic acid, 4-O-metilglicurônico acid and α -D-galacturonic) [5].

Classical methods for the determination of sugars in biomass are based on chromatographic technique, but in recent years the chemically modified electrodes have been developed for the determination of sugars. Several studies about non-enzymatic glucose sensors describe the use of gold electrodes. The electrocatalytic behavior of the glucose oxidation onto gold surface is highly complex, for all that, many investigations studied these mechanisms. But some aspects remain undefined, although a variety of mechanisms for this reaction has been suggested [6, 7].

Chemically modified carbon electrodes have appeared for use in the electrocatalytic oxidation of glucose and other sugars. The carbon electrodes developed explored the possibility of using carbon for the glucose oxidation sensors in order to manufacture at low cost. Generally the carbon substrates are used due to its electronic conductivity and other properties relevant [8, 9]. The appearing of carbon-based nanostructured materials, such as carbon nanotubes (CNT) and graphene, which improved the electrochemical detection of sugars. These materials are promising precursor materials for sensors due to ease of modification and functionalization, good conductivity, biocompatibility and large surface area [10, 11].

Many efforts have been made to find new precursor materials for electro-oxidation of glucose and sugars such as: porphyrin copper (II) [12], nickel oxide [13-15], cooper hydroxide [16], nickel hydroxide [17], Ni(II)-quercetin complex modified with multi-wall carbon nanotube and ionic liquid [18], nickel and multi-walled carbon nanotubes [19, 20], nickel and manganese oxides nanoparticles [21], multi-walled carbon nanotubes decorated with nickel and copper nanoparticles [22], nickel oxy-hydroxide [23], porous nickel-decorated single-walled carbon nanotubes [24], nickel/cobalt alloys [25], boron-doped carbon-coated nickel [26], Ni(II) ion, quercetin and grapheme [27], nickel electrodes plated with gold [28], poly(1-naphthylamine)/nickel [29], carbon nanotubes with NiCo-oxide [30] and glassy-carbon electrode modified with carbon nanotubes [31].

The electrodes modified with nanotubes containing metal oxides have anodic peak currents larger than the electrodes modified only with metal oxides, due to the high surface area, excellent electric conductivity, good mechanical properties and outstanding ability to promote electron-transfer reactions of the electrode in the presence of carbon nanotubes [14, 32, 33].

The study of the rate constants (k) for the reaction of sugars is important analytically because it is easily measure the kinetics of the process the redox couple between nickel and sugars, a high value of k reaches equilibrium in a very short time interval while a system with a low k takes a long time to reach equilibrium, the ease of reaching the equilibrium in short time interval with a gain of sensitivity and catalytic current increase is attributed to multiple walled carbon nanotubes, due to the gain area surface.

The scope of this work is the detailed research of oxidation of sugars in order to elucidate the kinetics of this electrochemical reaction. The electrocatalytic oxidation of sugars on the two types of electrodes is attractive because of the interest of building sensors for sugars for the production of second generation ethanol. In this work, a direct electrochemical oxidation of sugars in alkaline medium using multi-walled carbon nanotubes (MWCNTs) with nickel oxy-hydroxide modified glassy

carbon electrode (GC/MWCNT/NiOOH) and nickel oxy-hydroxide modified glassy carbon electrode (GC/NiOOH) to improve its electroactivity towards several sugars (glucose, galactose, mannose, arabinose and xylose). Morphology studies were performed electrode using scanning electron microscope (SEM). Redox properties and electron transfer behavior of these modified electrodes were investigated using cyclic voltammetry (CV). Direct electrochemical oxidation and rate constant values for the electrocatalytic oxidation reactions of sugars in alkaline medium were investigated using CV and chronoamperometry.

2. EXPERIMENTAL

2.1. Reagents

All reagents were of analytical grade (Sigma-Aldrich of Germany) and water was deionized using the Milli-Q Gradient system of Millipore. Multi walled carbon nanotubes with 95 % purity were supplied by (Dropesens-Spain). Nickel (II)-nitrate, N,N-Dimethylformamide, glucose, galactose, mannose, arabinose and xylose were obtained Sigma-Aldrich. The sugars solutions were prepared just prior to use.

2.2. Instrumentation

2.2.1. Electrochemical apparatus

Cyclic voltammetry measurements were made using a Autolab PGSTAT-30 potentiostat/galvanostat controlled by General Purpose Electrochemical System (GPES) software (Eco Chemie B.V.) equipped with a conventional three-electrode cell at room temperature. A GC-modified electrode with a 0.070 cm^2 surface area, an Ag/AgCl (KCl, 3.0 mol L^{-1}) electrode and platinum wire ($3.0\text{ cm} \times 0.1\text{ cm}$), were used as the working, reference and auxiliary electrodes, respectively. Before all electrochemical experiments, the electrochemical cell was saturated with nitrogen for 15 min.

2.3. Procedures

2.3.1. Electrode modification

The surface of the GC was polished with $0.3\text{ }\mu\text{m}$ alumina powder (Merck) and cleaned by sonication in ethanol and Milli-Q water for 3 min. 10.0 mg MWCNT was dispersed in 10.0 mL N,N-dimethylformamide (DMF) with an ultrasonic bath to give a 1.0 mg mL^{-1} black solution. $35\text{ }\mu\text{L}$ of the black solution was casting at the GC electrode surface to prepare the GC/MWCNT electrode surface. Modification of the electrode was accomplished by transferring $10\text{ }\mu\text{L}$ of aqueous $2 \times 10^{-3}\text{ mol L}^{-1}$ nickel nitrate solution to the CG/MWCNT electrode surface, at the end of each step, the electrode was allowed dry at $50\text{ }^\circ\text{C}$ for 20 min, the electrode was described by CG/MWCNT/NiOOH. $10\text{ }\mu\text{L}$ of the aqueous $2 \times 10^{-3}\text{ mol L}^{-1}$ nickel nitrate solution to the CG electrode surface, the electrode was allowed to dry at $50\text{ }^\circ\text{C}$ for 20 min and the electrode was described by CG/NiOOH. The electrodes were

conditioned by potential cycling in a limited range (0.1 - 0.6 V vs. Ag/AgCl) in 0.10 mol L⁻¹ NaOH solution, as supporting electrolyte, until a steady state of current was obtained. The GC/MWCNT/NiOOH and GC/NiOOH electrodes were used for study of glucose, galactose, mannose, arabinose and xylose oxidation.

2.3.2. Voltammetric measurements

The GC/NiOOH and GC/MWCNT/NiOOH were characterized by cyclic voltammetry (CV). The influence of scan rate on the GC/NiOOH and GC/MWCNT/NiOOH were performed between 10 and 700 mV s⁻¹ in the potential range of 0.1 to 1.0 V in a solutions of 0.1 mol L⁻¹ NaOH. All experiments were performed at room temperature 25 °C.

2.3.3. Electrochemical behavior of GC/NiOOH and GC/MWCNT/NiOOH in presence of sugars.

GC/NiOOH and GC/MWCNT/NiOOH electrodes were applied to sugars electrochemical experiments in an electrochemical cell with 10 mL of 0.1 mol L⁻¹ NaOH solution. All experiments were done in triplicate. The CV technique was employed to study the electrochemical behavior. The catalytic current was estimated from the difference between the current measured in absence and presence of sugars. Chronoamperometry were carried out in 0.1 mol L⁻¹ NaOH solution containing 0.025 mol L⁻¹ of sugars, the oxidation potential was applied 0.6 V vs. Ag/AgCl.

2.3.4. Characterization by scanning electron microscopy.

GC/MWCNT/NiOOH electrode was characterized using a scanning electron microscope with cannon electron emission field (SEM-FEG) of Brand Jeol, JSM 7500F model. For the analysis of the modified electrodes were used glassy carbon plates with a total area of 1.0 cm² and a thickness of 0.2 cm with a covered area of 0.070 cm².

3. RESULTS AND DISCUSSION

3.1. Electrochemical behavior of the modified electrodes.

Initially some parameters on the surface of glassy carbon electrode were optimized. From studies of volume and concentration of carbon nanotubes suspensions used in preparation of electrodes the optimized conditions were 35 μL of 1.0 mg mL⁻¹ of nanotubes/DMF and 10 μL of 2.0×10⁻³ mol L⁻¹ of nitrate nickel. Figure 1 shown the electrochemical behavior of the GC, GC/NiOOH and GC/MWCNT/NiOOH in 0.1 mol L⁻¹ NaOH. It were observed two current peaks that corresponding to the anodic (E_{pa}) and cathodic (E_{pc}) redox couple Ni^(II)/Ni^(III) [34, 35], at 0.49 V and 0.35 V, respectively. Equation 1 corresponds to redox process of the GC/NiOOH.



The figure 1-A show cyclic voltammograms of the GC/MWCNT/NiOOH exhibit a couple of peaks with E^0 ($E_{pa} + E_{pc} / 2$) and ΔE_p of 0.43 V and 0.15 V respectively with scan rate of 50 mV s^{-1} . Although the anodic and cathodic potential peaks exhibited values close for both GC/NiOOH and GC/MWCNT/NiOOH electrodes, the anodic and cathodic peak current of the GC/MWCNT/NiOOH showed much higher values when compared to the GC/NiOOH electrode. These relative increases of peak currents are probably resulting from increased surface area provided by carbon nanotubes onto surface of GC/MWCNT/NiOOH [14, 33].

The surface coverage of the electrode (Γ) could be evaluated from the area under the anodic peak of the CV (Q) for the GC/NiOOH and GC/MWCNT/NiOOH electrodes. This is defined by the following equation [36]:

$$\Gamma = \frac{Q}{nFA} \quad (2)$$

where n is the number of electrons, F is the constant of Faraday and A is the area of the surface of the GC electrode.

The value of $4.3 \times 10^{-8} \text{ mol cm}^2$ was found to GC/NiOOH and $3.2 \times 10^{-7} \text{ mol cm}^2$ to GC/MWCNT/NiOOH, this may indicate that in the presence of carbon nanotubes the species of nickel are more distributed across on electrode surface and it can be cause of peak current increases in the GC/MWCNT/NiOOH electrode.

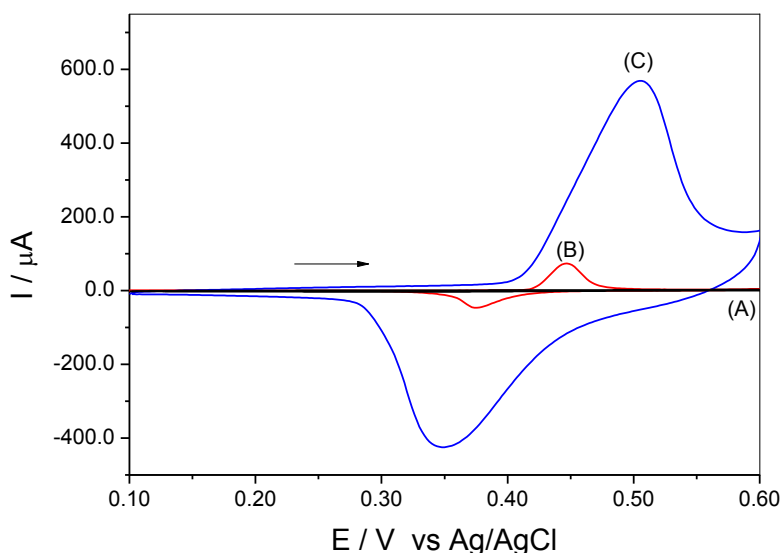


Figure 1. Cyclic voltammograms of (A) GC, and (B) GC/NiOOH and (C) GC/MWCNT/NiOOH electrodes ($0.1 \text{ mol L}^{-1} \text{ NaOH}$; $\nu = 50 \text{ mV s}^{-1}$).

The Figure 2-A and Figure 3-A show cyclic voltammograms of the GC/NiOOH and GC/MWCNT/NiOOH at different scan rates from 2 to 700 mV s^{-1} in 0.1 NaOH in the potential range from -0.1 to 1.0 V . We observed a separation of peak potentials that increased with higher scan rates. In according to literature [37, 38] these results indicate a limitation in the charge-transfer kinetics attributed to various factors, such as chemical interactions between the electrolyte ions and the modified electrode, dominance of electrostatic factors, adjacent interactions of the redox couples present on the electrode surface and non-equivalent sites present in the modified electrode.

The electron transfer kinetics at GC/NiOOH and GC/MWCNT/NiOOH electrodes has also been studied. Laviron derived general expressions for the case of surface-confined electro-reactive species at small concentrations and it is possible to determine the charge transfer coefficient, α , and the heterogeneous electron transfer rate constant, k_s , by measuring the variations of the peak potentials as a function of the scan rate. The ΔE_p increases to a very little extent, when the scan rate is increased from 2 to 200 mV s^{-1} . However, at higher scan rates ($>200 \text{ mV s}^{-1}$), the peak separation is found to be larger indicating the limitation arising from the charge transfer kinetics [39].

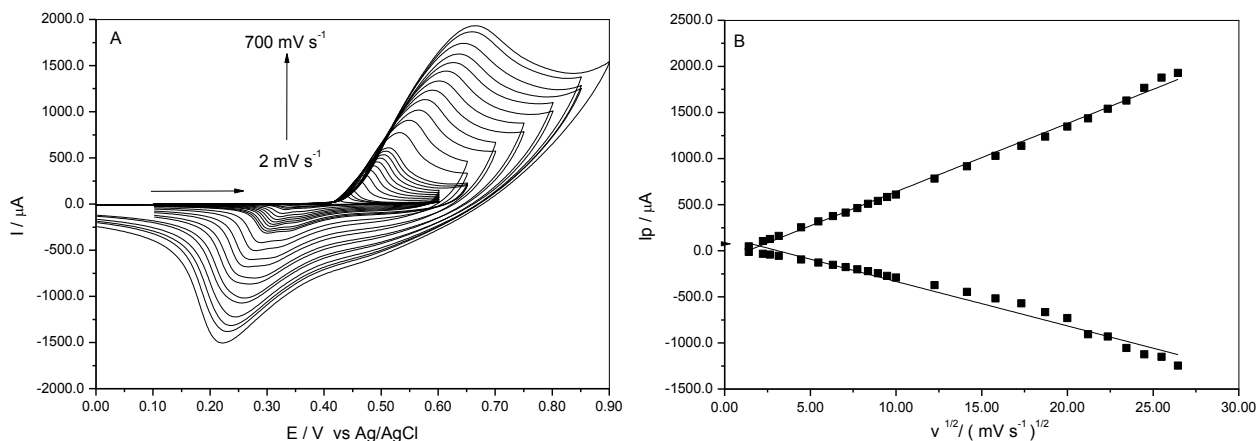
Figure 2-B and 3-B show the relationship of current peak versus scan rates from 0 to 700 mV s^{-1} . Both the anodic and the cathodic peak currents were proportional to the square root of scan rate indicating a diffusion controlled process for GC/NiOOH and GC/MWCNT/NiOOH [36, 39].

However, the peaks currents are proportional to scan rates in the range of 2 to 100 mV s^{-1} , pointing to the electrochemical activity controlled by adsorption[36, 39]. A plot of E_p vs. $\log v$ (Figure 2-C and 3-C) yields two straight lines with slopes of $-2.3 RT/\alpha nF$ for the cathodic peak and $2.3 RT/(1-\alpha)nF$ for the anodic peak. Since known the value of n and from these expressions α can be determined by slope the variation of the peak potential with respect to the potential scan rates shown in Figure 2-C and 3-C. Under these conditions, the following equation can be used to determine the electron transfer rate constant (k_s) of the GC electrode with GC/NiOOH and/or GC/MWCNT/NiOOH electrodes:

$$\log k_s = \alpha \log(1-\alpha) + (1-\alpha) \log \alpha - \log (RT/nFv) - \alpha(1-\alpha) nF \Delta E_p/2.3RT \tag{3}$$

where $n = 1$, $\Delta E_p = E_{pa} - E_{pc}$, v is the scan rate and all other symbols have their usual meanings [38].

The calculated values of the k_s and α for GC/NiOOH were about 0.18 s^{-1} and 0.76 , for GC/MWCNT/NiOOH calculated values of the k_s and α were about 0.10 s^{-1} and 0.85 , respectively. When comparing the values of k_s between GC/NiOOH and GC/MWCNT/NiOOH is noted that GC/NiOOH has higher value, it is because that k_s is a measure of the electronic transfer between GC and NiOOH, as the GC/NiOOH electrode has no carbon nanotubes this electronic transfer is easier and faster be performed.



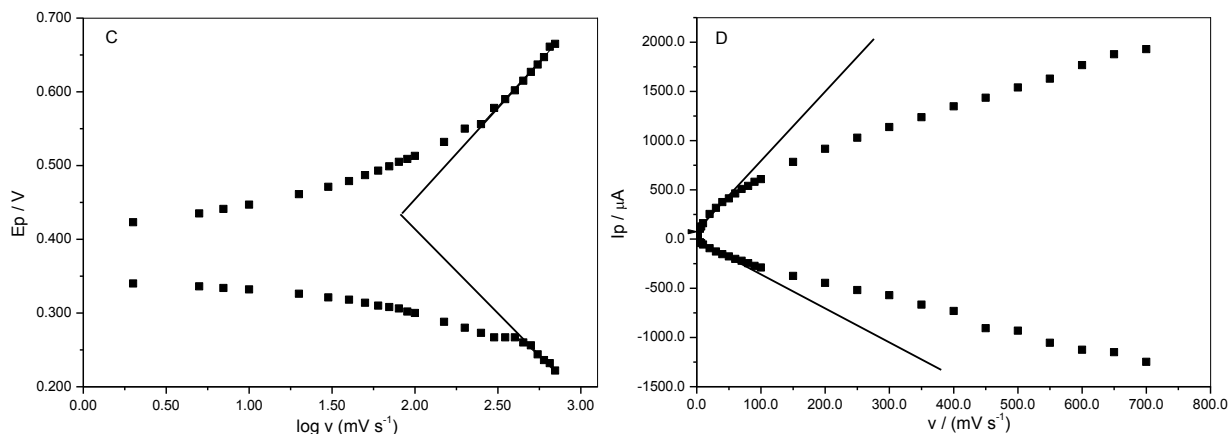
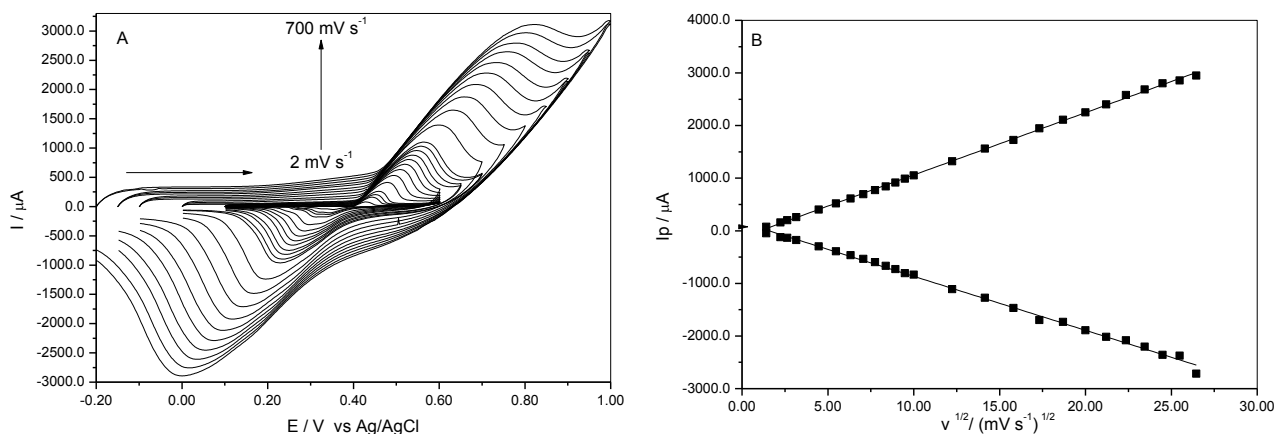


Figure 2. (A) Cyclic Voltammograms of GC/NiOOH electrode in 0.1 mol L⁻¹ NaOH. Potential scan rates from inner to outer are: 2, 5, 7, 10, 20, 30, 40, 50, 60, 70, 80, 90, 100, 150, 200, 250, 300, 350, 400, 450, 500, 550, 600, 650 and 700 mV s⁻¹. (B) The dependency of anodic (I_{pa}) and cathodic (I_{pc}) peak currents on the square roots of scan rates at values of 2-700 mV s⁻¹. (C) Plot of E_p versus $\log v$ for cyclic voltammograms depicted in (A) for anodic (E_{pa}) and cathodic (E_{pc}) peaks potential. (D) The dependency of anodic (I_{pa}) and cathodic (I_{pc}) peak currents on the potential scan rates at values of 2-700 mV s⁻¹.

3.2. Microscopic characterization.

The glassy carbon electrode with carbon nanotubes (GC/MWCNT) and GC/MWCNT/NiOOH were analyzed by comparing the topography of surfaces at different magnifications of the images of micrographs generated by SEM-FEG. The electrodes were prepared by cyclic voltammetry in the potential range from 0.1 to 0.7 V vs. Ag/AgCl in solution 0.1 mol L⁻¹ NaOH ($v = 50 \text{ mV s}^{-1}$).

Figures 4-A and 4-B show the SEM micrographs with magnifications of 20,000 and 200,000 times for the GC/MWCNT electrode. In accordance to Figures 4-A and 4-B, we observed that the carbon nanotubes are fully dispersed on the surface of CG showing a total coating of the GC surface and Figure B shows the details of the carbon nanotubes and estimated its size, which has a diameter around of 11 nm, which is consistent with the data sheet is issued by the manufacturer.



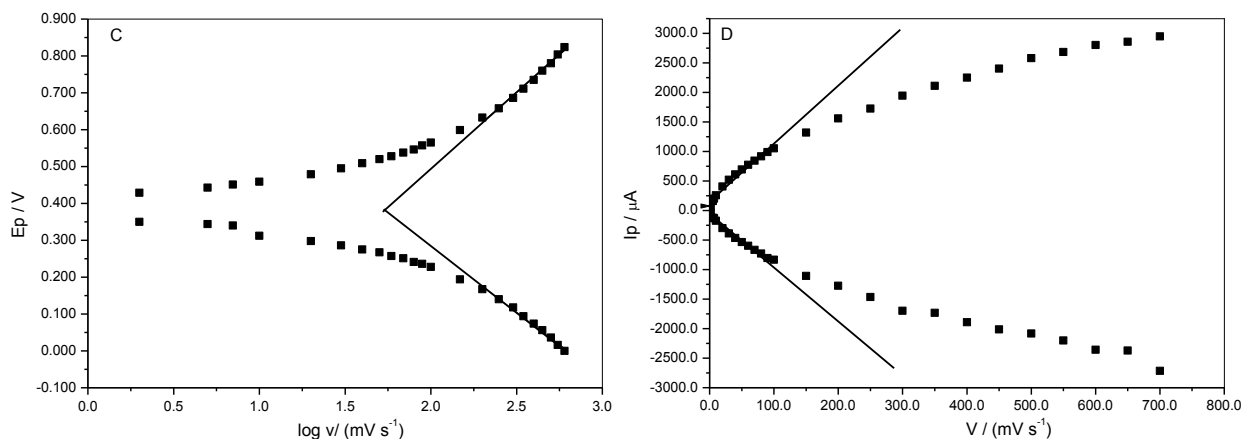


Figure 3. (A) Cyclic Voltammograms of GC/MWCNT/NiOOH electrode in 0.1 mol L⁻¹ NaOH. Potential scan rates from inner to outer are: 2, 5, 7, 10, 20, 30, 40, 50, 60, 70, 80, 90, 100, 150, 200, 250, 300, 350, 400, 450, 500, 550, 600, 650 and 700 mV s⁻¹. (B) The dependency of anodic (I_{pa}) and cathodic (I_{pc}) peak currents on the square roots of scan rates at values of 2-700 mV s⁻¹. (C) Plot of E_p versus log v for cyclic voltammograms depicted in (A) for anodic (E_{pa}) and cathodic (E_{pc}) peaks potential. (D) The dependency of anodic (I_{pa}) and cathodic (I_{pc}) peak currents on the potential scan rates at values of 2-700 mV s⁻¹.

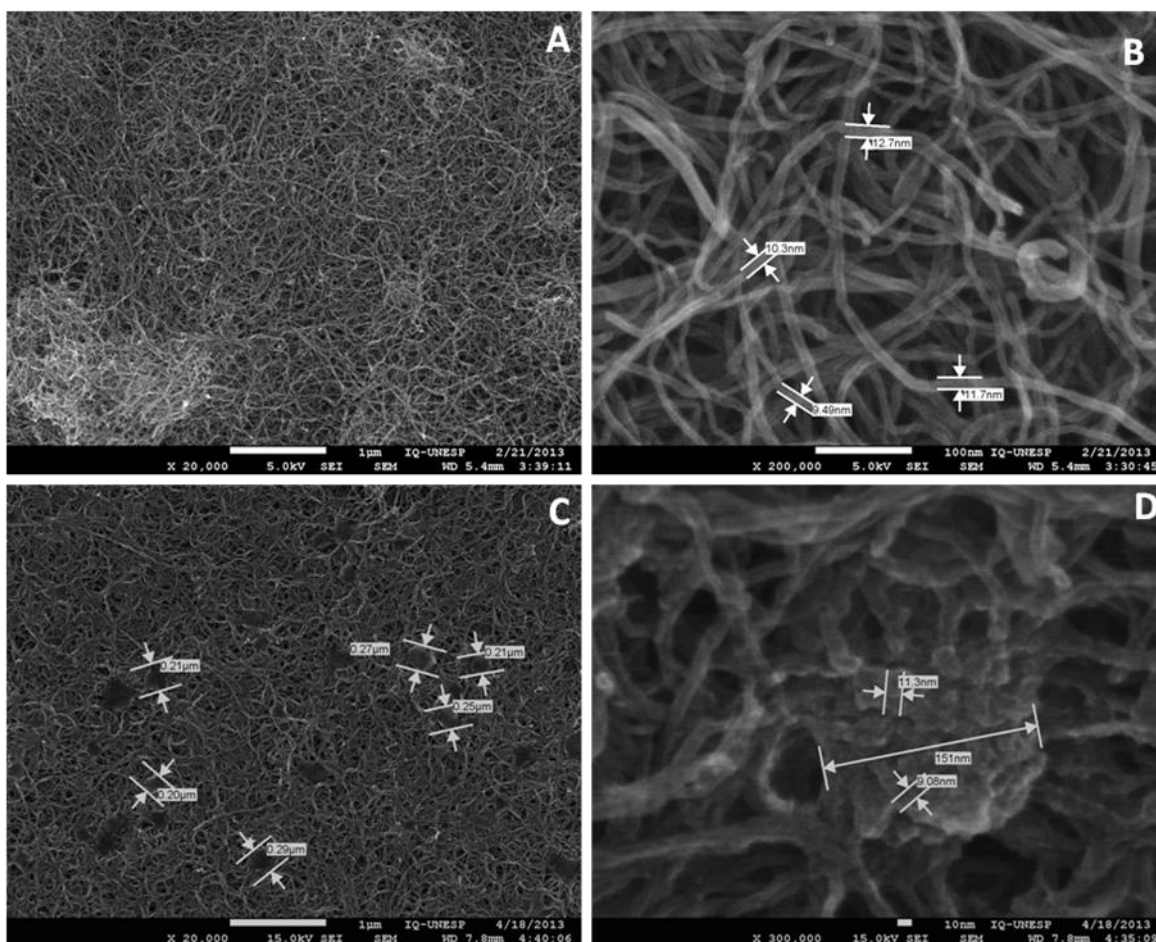


Figure 4. SEM images for carbon nanotubes (CG/MWCNT) with magnifications: (A) 10,000; (B) 20,000 and CG/MWCNT/NiOOH: (C) 200,000; (D) 300,000 times.

The modification of the GC/MWCNT/NiOOH electrode is shown in Figure 4 (C and D). The Figure 4-C shows where different particles size around of 0.25 μm are dispersed on the surface of the nanotubes. However, when analyzing the Figure 4-D is observed that the average size of nanoparticles of 10 nm agglomerates forming a single particle. An indication of the successfully modification of the GC/MWCNT/NiOOH electrode is illustrated in Figure 5 by the EDS spectrum where peaks of nickel and oxygen were observed indicating that the nickel particles formed were species of oxides of nickel.

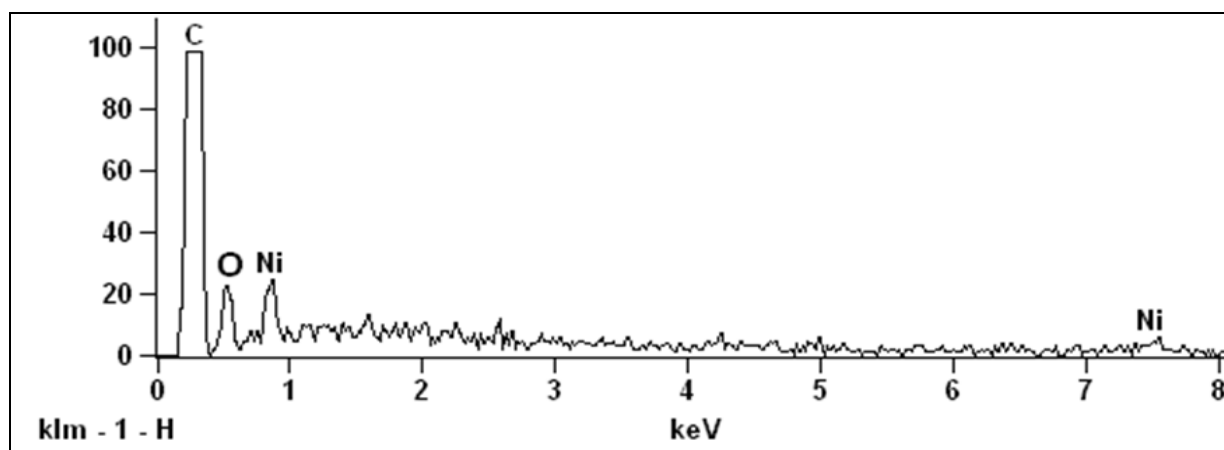


Figure 5. EDS spectrum of the GC/MWCNT/NiOOH with accelerating voltage of 7.0 kV.

3.3. Electro-oxidation of sugars

The electro-oxidation of sugars in the glassy carbon electrode without modification was studied by cyclic voltammetry. In Figure 6 (A) is shown the electro-oxidation of galactose, which requires higher potentials around 1.2 V vs. Ag/AgCl. The electro-oxidation of galactose on electrodes modified GC/NiOOH and GC/MWCNT/NiOOH as shown in the Figure 6 (B and C) occurred at lower potentials about 0.55 V vs. Ag/AgCl associated with increased anodic peak current and decrease in cathodic peak current, however there is a small peak at around 0.45 V in Figure 6-C (II), was observed that this peak is not pronounced in the modification of the electrode with lower volumes of carbon nanotubes, this is an indication that the sugar is adsorbed on the surface of the nanotubes also and as a consequence the appearance of this peak at 0.45 V. For the others sugars we observed the same behavior (data not showed). The results suggest that $\text{Ni}^{(\text{II/III})}$ can catalyze the electro-oxidation of galactose to galactonolactone, according to the reactions 4 and 5 [40], the reaction of oxidation for the other sugars are similar [35, 41-44].



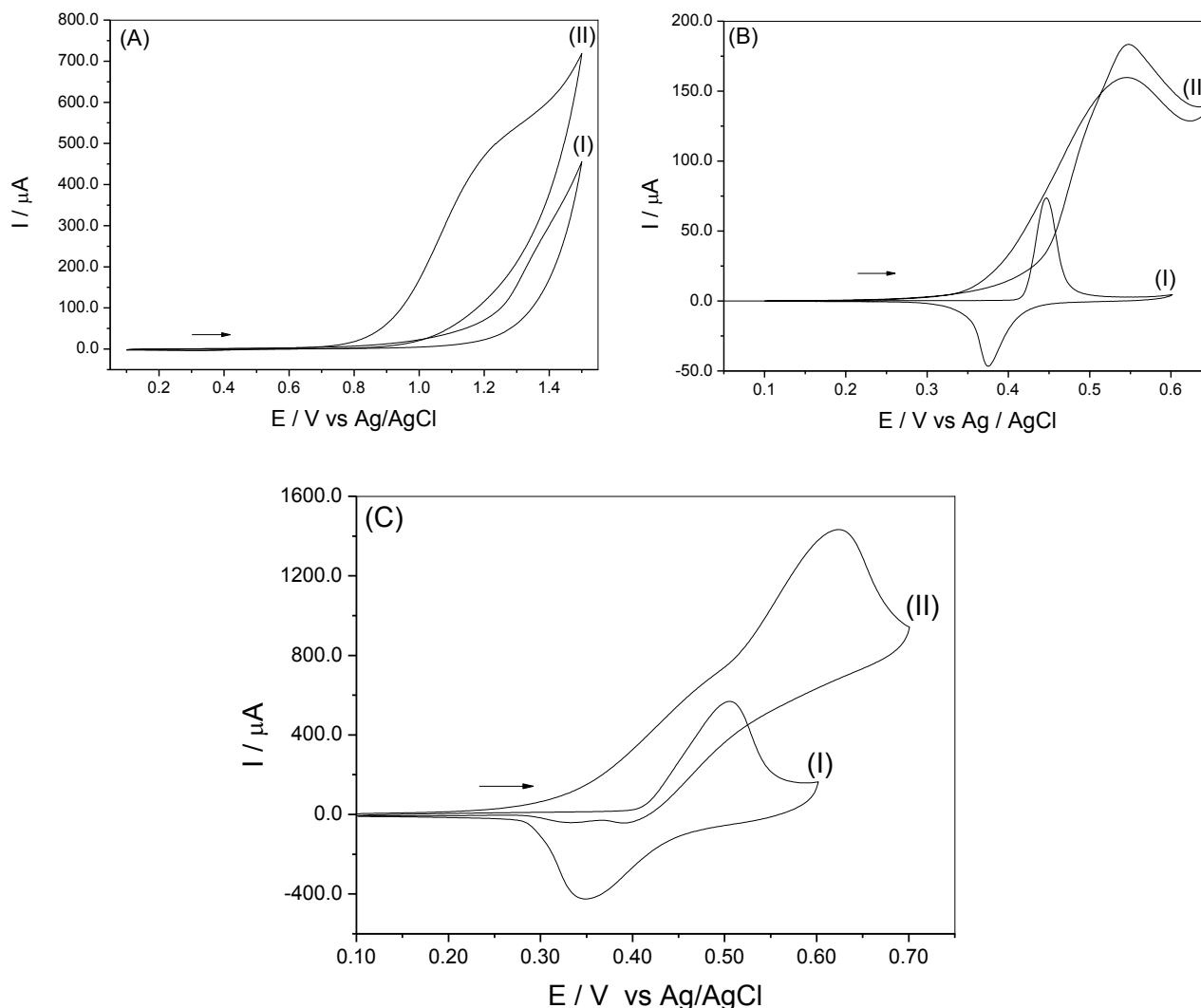


Figure 6. Cyclic voltammograms containing the electro-oxidation of (I) absence and (II) presence of 0.01 mol L^{-1} in galactose: (A) GC electrode; (B) GC/NiOOH electrode; (C) GC/MWCNT/NiOOH electrode (0.1 mol L^{-1} NaOH; 50 mV s^{-1}).

Figure 7-A shows the cyclic voltammograms of the scan rates studies of the GC/MWCNT/NiOOH electrode in the presence of 0.01 mol L^{-1} galactose. It was observed that the peak potential for the catalytic oxidation of galactose shifts to increasingly positive potential with increasing scan rate, this result suggests limiting kinetics of reaction between the redox sites of the electrode GC/MWCNT/NiOOH and galactose. The Figure 7-B shows that the anodic peak current is proportional to the square root of the scan rate indicating a process of mass transfer controlled by diffusion [36, 38] according to the equation $I_{pa} = -2.50 \times 10^{-5} + 2.24 \times 10^{-4} v^{1/2}$, and a correlation coefficient of 0.994. It is also observed in Figure 7-C a relationship between the function $Iv^{-1/2}$ and v , where it is observed a behavior corresponding to an electrochemical and chemical process (EC) [14]. All studies of the influence of scan rate were made for the other sugars (arabinose, glucose, mannose and xylose) and behaviors were similar.

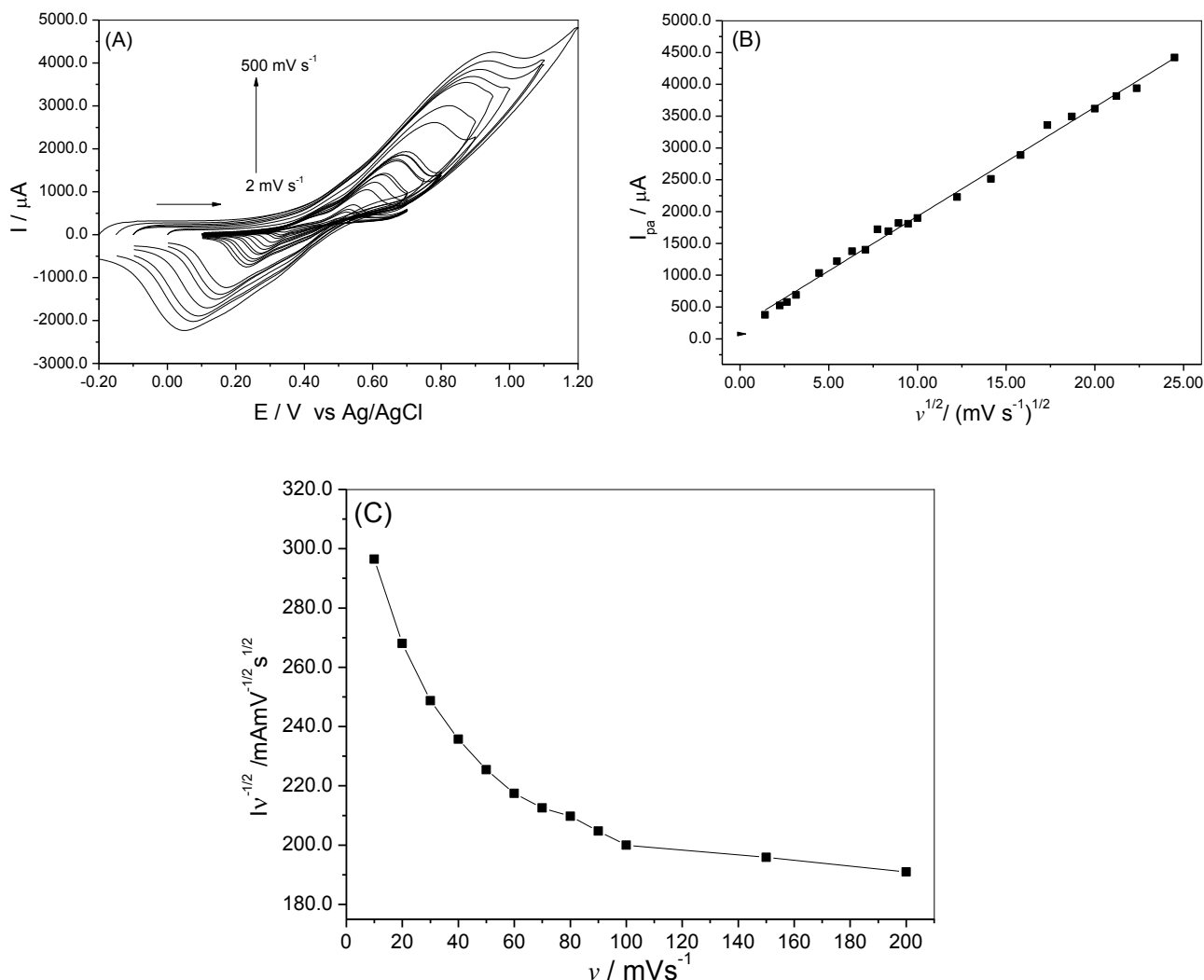


Figure 7. (A) Cyclic Voltammograms of GC/MWCNT/NiOOH electrode in 0.01 mol L⁻¹ galactose (0.1 mol L⁻¹ NaOH. Potential scan rates from inner to outer are: 2, 5, 7, 10, 20, 30, 40, 50, 60, 70, 80, 90, 100, 150, 200, 250, 300, 350, 400, 450 and 500 mV s⁻¹. (B) The dependency of anodic peak (I_{pa}) currents on the square roots of scan rates at values of 2-500 mV s⁻¹. (C) Plots of anodic current function (Iv^{-1/2}) vs. the scan rates (v).

3.4. Kinetic study of electrocatalytic oxidation of sugars

Equations can be represented by the following half-reactions:



where galactose is the electroactive kind in its reduced form, galactonolactone is the electroactive species in its oxidized form and k is the electrocatalytic rate constant. Considering the exponential dependence of k with overpotential [45-49] the reaction rate of the electrochemical process, j, is given by the Equation 7.

$$j = k_f [\text{galactose}^{\text{red}}]^{\nu} \exp\left(\frac{\alpha n F \eta}{RT}\right) - k_b [\text{galactonolactone}^{\text{ox}}]^{\nu} \exp\left[\frac{-(1-\alpha)nF\eta}{RT}\right] \quad (7)$$

Under the condition of high field ($n > 0.1$ V), the cathodic component of the Equation 7 becomes negligible, resulting in the following expression:

$$j = k_f [\text{galactose}^{\text{red}}]^{\nu} \exp\left(\frac{\alpha n F \eta}{RT}\right) \quad (8)$$

where k_f is the rate constant in the anodic direction, α is the coefficient of transfer (or factor symmetric), $[\text{galactose}^{\text{red}}]$ is the concentration of electroactive species on electrode surface, and ν is the reaction order corresponding to galactonolactone species. The resignation symbols are usual, linearizing the Equation 8 has:

$$\ln j = \ln k_f + \nu \ln [\text{galactose}^{\text{red}}] + \frac{\alpha n F \eta}{RT} \quad (9)$$

Considering that the Tafel curve has the form E vs. $\log j$, and that coefficient of Tafel, b , is defined as straight angled coefficient, which has the Equation 9 must be rearranged in order to obtain dependency E vs. $\log j$, which is given by the following expression:

$$E = E^{\circ} + \frac{2,303RT(\log j - \log k_f - \nu \log [\text{galactose}^{\text{red}}])}{\alpha n F} \quad (10)$$

Equation 10 shows that the values of b should be calculated from the relationship of E vs. $\log j$ according to the partial derivative:

$$b \equiv (\partial E / \partial \log j)_{T, [\text{galactose}]} \quad (11)$$

Applying the definition Tafel coefficient is given by:

$$b = \frac{2,303RT}{\alpha F} \quad (12)$$

Figure 8 shows Tafel curves for the GC/NiOOH and GC/MWCNT/NiOOH electrodes that were recorded in 0.1 mol L^{-1} NaOH in the presence of 0.01 mol L^{-1} of galactose with $\nu = 10 \text{ mV s}^{-1}$. The Tafel slopes and electron-transfer coefficients for sugars under study are presented in Table 1.

The reaction kinetics of the oxidation of sugars with the redox sites of the GC/NiOOH and GC/MWCNT/NiOOH electrodes were investigated by chronoamperometry according to Equation 13 [36, 38].

$$\frac{I_{\text{catal}}}{I_d} = \lambda^{1/2} \left[\pi^{1/2} \text{erf}(\lambda^{1/2}) + \frac{\exp(-\lambda)}{\lambda^{1/2}} \right] \quad (13)$$

where I_{catal} is the catalytic current in the presence of sugar, I_d the limiting current in the absence of sugar and $\lambda = kCt$ (k , C and t are the electrocatalytic rate constant, bulk concentration of sugar and the elapsed time, respectively) is the argument of the error function. For $\lambda > 1.5$, $\text{erf}(\lambda^{1/2})$ almost equals unity and equation 13 reduces to:

$$\frac{I_{\text{catal}}}{I_d} = \lambda^{1/2} \pi^{1/2} = \pi^{1/2} (kCt)^{1/2} \quad (14)$$

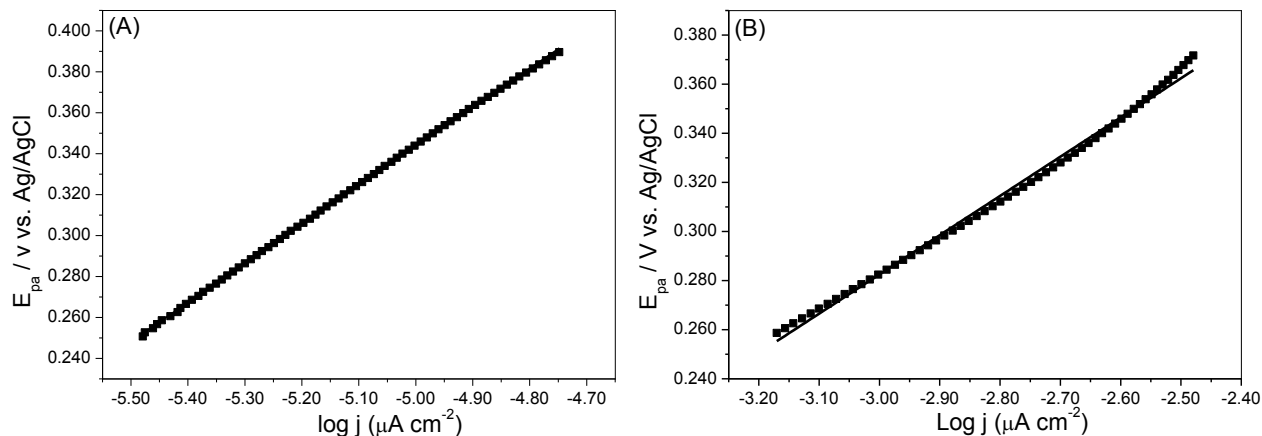


Figure 8. Representative Tafel curves (A) GC/NiOOH electrode and (B) GC/MWCNT/NiOOH electrode in 0.01 mol L^{-1} galactose ($\nu = 10 \text{ mV s}^{-1}$; 0.1 mol L^{-1} NaOH).

From the slope of the $I_{\text{catal}}/I_{\text{d}}$ plot the value of k at a given concentration of sugar is derived. The k and D values for studies at a concentration of $2.5 \times 10^{-2} \text{ mol L}^{-1}$ sugars are shown in Table 1. Figure 9 show chronoamperograms of all sugars. The values of the diffusion coefficient were obtained through the Randles-Sevcik equation (Eq. 15) for irreversible systems by scan rates study with sugars concentration of 0.01 mol L^{-1} :

$$i_p = (2,99 \times 10^5) \alpha^{1/2} A C^* D^{1/2} \nu^{1/2} \quad (15)$$

where: A is the electrode area (cm^2); C is the bulk concentration of sugars (mol cm^{-3}); D is the diffusion coefficient ($\text{cm}^2 \text{ s}^{-1}$); ν is the scan rate (V s^{-1}).

According to Table 1, it was possible to compare kinetic parameters of the GC/NiOOH with GC/MWCNT/NiOOH. We observed higher values of sugars electrocatalytic rate constants for GC/MWCNT/NiOOH, it is probably due resulting from a larger area surface provided by carbon nanotubes on modified surface of GC/MWCNT/NiOOH electrode [14, 33].

It is shown in Table 1 electrocatalytic reaction rate constant, a difference of k observed between different sugars could be attributed to the difficulty of adsorption on the GC/NiOOH and GC/MWCNT/NiOOH. For undergoing electrochemical oxidation these molecules have to get adsorbed on the electrode surface, the number of electrons transferred during oxidation of sugars and very high due to the formation of different intermediates that are also oxidized on the surface of highly catalytic electrodes. As reported by some authors [17, 50], oxidation of sugars on the surface of the electrodes is mainly performed by primary hydroxyl groups which can occur by formation of H-bonds between the OH groups and the nickel oxy-hydroxide layer, it was observed that for both GC/NiOOH and/or GC/MWCNT/ NiOOH the values of the rate constant for electrocatalytic glucose is higher, since these groups are more readily available for oxidation and exhibit the highest values of k because of their high reducing powers. The variation in the values of k and Tafel slopes can be attributed to the change of the adsorption process of carbohydrates and intermediates products onto the electrode surface due to change in the surface structure after the electrode modification process [52, 53].

Table 1. Values of electronic transfer coefficient (α), electrocatalytic rate constant (k) and diffusion coefficient (D) for all the sugars in the study with GC/NiOOH and GC/MWCNT/ NiOOH electrodes.

Sugars	GC / NiOOH				GC / MWCNT / NiOOH			
	Tafel slope (mV decade ⁻¹)	α	D (cm ² s ⁻¹)	k (mol L ⁻¹)	Tafel slope (mV decade ⁻¹)	α	D (cm ² s ⁻¹)	k (L mol ⁻¹ s ⁻¹)
Glucose	184.1	0.32	1.7×10^{-7}	1.3×10^3	128.3	0.46	1.5×10^{-6}	4.3×10^4
Galactose	190.5	0.31	1.5×10^{-7}	1.1×10^3	159.7	0.37	1.3×10^{-6}	2.1×10^4
Mannose	163.0	0.21	5.9×10^{-8}	8.3×10^2	262.1	0.22	2.8×10^{-6}	1.4×10^4
Arabinose	221.0	0.26	3.9×10^{-8}	8.9×10^2	215.0	0.27	2.0×10^{-6}	2.1×10^4
Xylose	175.2	0.22	1.6×10^{-7}	8.3×10^2	251.8	0.23	3.0×10^{-6}	2.0×10^4

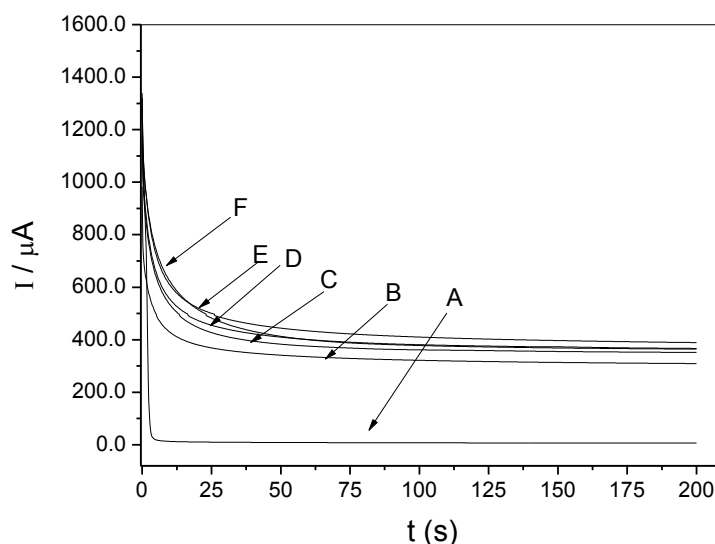


Figure 9. Chronoamperograms of the GC/MWCNT/NiOOH electrode in 0.1 mol L⁻¹ NaOH in the absence (A) and presence of 25×10^{-3} mol L⁻¹ of mannose (B), xylose (C), arabinose (D), galactose (E) and glucose (F). Applied potential 550 mV.

Table 2. The comparison of the electrocatalytic reaction rate constant (k) of the GC/MWCNT/NiOOH electrode with the reported Chemical Modified Electrodes (CMEs).

Chemically Modified Electrodes basead on	Sugars	k (L mol ⁻¹ s ⁻¹)	reference
Nickel (II) – quercetin complex modified multiwall carbon nanotube ionic liquid	Glucose	1.91×10^3	18
Immobilization of glucose oxidase on electrodeposited nickel oxide nanoparticles	Glucose	1.1×10^4	51
Nickel (II), quercetin and graphene	Glucose	2.93×10^3	27
Poly(1-naphthylamine)/nickel	Glucose	0.229	29
Poly(1-naphthylamine)/nickel	Galactose	0.275	29
GC/MWCNT/NiOOH	Glucose	4.36×10^4	This work
GC/MWCNT/NiOOH	Galactose	2.09×10^4	This work

3.5. Study of concentration of sugars

The study of concentration of sugars were carried out in the concentration range of 5.0×10^{-5} to 1.4×10^{-2} mol L⁻¹ in 0.1 mol L⁻¹ NaOH solution with scan rate of 50 mV s⁻¹. It has been observed that the increase of anodic peak current is linear with the increase of concentration of sugars. For galactose, a linear dependence was observed in a concentration range from 2.5×10^{-4} to 5.6×10^{-3} mol L⁻¹ according to the equation $I_{pa} = 1.42 \times 10^{-5} + 0.14 \times [\text{galactose}]$ and correlation coefficient of 0.999. At higher concentrations the analytical response shows a deviation in linearity, probably due to saturation of the active sites on the surface of GC/MWCNT/NiOOH

The Table 3 shows the electrochemical parameters for all sugars studied. We observed that the electrode GC/MWCNT/NiOOH has good sensitivity amperometric. The values of limit of detection and quantification are very close, meaning that the behaviors of sugars on the electrode are similar.

Table 3. Analytical parameters for various sugars at GC/MWCNT/NiOOH in 0.1 mol L⁻¹ NaOH by CV ($v = 50$ mV s⁻¹; $n = 3$).

Sugars	Limit of Detection (mol L ⁻¹)	Limit of Quantification (mol L ⁻¹)	Sensitivity ($\mu\text{A L mol}^{-1}$)	Concentration range (mol L ⁻¹)
Arabinose	2.6×10^{-4}	8.8×10^{-4}	1.1×10^5	5.0×10^{-4} - 5.6×10^{-3}
Galactose	2.1×10^{-4}	7.0×10^{-4}	1.4×10^5	2.5×10^{-4} - 5.6×10^{-3}
Glucose	1.9×10^{-4}	6.4×10^{-4}	1.3×10^5	2.5×10^{-4} - 5.6×10^{-3}
Mannose	4.3×10^{-4}	1.4×10^{-3}	1.5×10^5	5.0×10^{-4} - 5.6×10^{-3}
Xylose	3.2×10^{-4}	1.0×10^{-3}	9.1×10^4	5.0×10^{-4} - 5.6×10^{-3}

4. CONCLUSION

This work presents the simple preparation and usefulness of carbon nanotube modified with nickel oxy-hydroxide electrode for sugars electro-oxidation in alkaline media. Kinetic parameters for oxidation of sugars were calculated using cyclic voltammetry and chronoamperometry. We observed that higher catalytic currents were always obtained for the electro-oxidation of sugars at the GC/MWCNT/NiOOH electrode as compared to those obtained using GC/NiOOH. GC/MWCNT/NiOOH showed charge-transfer coefficient, catalytic reaction rate constant and diffusion coefficient in accordance to others electrodes described in literature. GC/MWCNT/NiOOH exhibited a linear current dependence on concentration of many sugars. This modified electrode proposed shown that it was a potential candidate for development of detectors to analytical applications in different samples.

ACKNOWLEDGEMENTS

The authors acknowledge financial support from the Fundação de Amparo à Pesquisa do Estado de São Paulo (FAPESP) (Processes 2011/19289-5; 2012/00258-5; 2011/20416-1)

References

1. C. A. Cardona, J. A. Quintero and I. C. Paz, *Bioresour. Technol*, 101 (2010) 4754
2. J. B. Sluiter, R. O. Ruiz, C. J. Scarlata, A. D. Sluiter and D.W. Templeton, *J. Agric. Food Chem*, 58 (2010) 9043
3. C. R. Soccol, L. P. S. Vandenberghe, A. B. P. Medeiros, S. G. Karp, M. Buckeridge, L. P. Ramos, A. P. Pitarelo, V. F. Leitão, L. M. F. Gottschalk, M. A. Ferrara, E. P. S. Bom, L. M. P. Moraes, J. A. Araujo and F. A. G. Torres, *Bioresour. Technol*, 101 (2010) 4820
4. E. Bahcegul, H. E. Toraman, N. Ozkanc and U. Bakir, *Bioresour. Technol*, 103 (2012) 440
5. F. M. Girio, C. Fonseca, F. Carvalheiro, L. C. Duarte, S. Marques, and R. Bogel-Lukasik, *Bioresour. Technol*, 101 (2010) 4775
6. L. D. Burke, *Electrochim. Acta*, 39 (1994) 1841
7. L. D. Burke, *Gold Bull*, 37 (2004) 125
8. S. A. Wring, J. Hart, L. Bracey and B. Birch, *Anal. Chim. Acta*, 231, (1990) 203
9. J. D. Newman, A. P. F. Tumer and G. Marrazza, *Anal. Chim. Acta*, 262 (1992) 13
10. X. Li, Q. Zhu, S. Tong, W. Wang and W. Song, *Sens. Actuators, B*, 136 (2009) 444
11. C. Hu and S. Hu, *J. Sensors*, (2009) 1
12. K. Sugawara, F. Yamamoto, S. Tanaka and H. Nakamura, *J. Electroanal. Chem*, 394 (1995) 263
13. S. Berchmans, H. Gomathi and G. Prabhakara Rao, *J. Electroanal. Chem*, 394 (1995) 267
14. M. Shamsipur, M. Najafi and M. R. M. Hosseini, *Bioelectrochemistry*, 77 (2010) 120
15. Y. Mu, D. Jia, Y. He, Y. Miao and H. L. Wu, *Biosens. Bioelectron*, 26 (2011) 2948
16. M. Jafarian, M. Rashvand avei, I. Danaee, F. Gobal and M. G. Mahjani, *Chin. J. Cat*, 31 (2010) 1351
17. M. Vidotti, C. D. Cerri, R. F. Carvalhal, J. C. Dias, R. K. Mendes, S. I. C. Torresi and L. T. Kubota, *J. Electroanal. Chem*, 636 (2009) 18
18. L. Zhenga, J. Zhang and J. Songa, *Electrochim. Acta*, 54 (2009) 4559
19. A. Suna, J. Zhenga and Q. Shenga, *Electrochim. Acta*, 65 (2012) 64
20. H. Nie, Z. Yao, X. Zhou, Z. Yang and S. Huang, *Biosens. Bioelectron*, 30 (2011) 28
21. S. M. El-Refaei, M. I. Awad, B. E. El-Anadouli and M. M. Saleh, *Electrochim. Acta*, 92 (2013) 460
22. K. C. Lin, Y. C. Lin and S. M. Chen, *Electrochim. Acta*, 96 (2013) 164
23. D. E. Pissinis, L. E. Sereno and J. M. Marioli, *J. Electroanal. Chem*, 694 (2013) 23
24. N. D. Dung, D. Patil, H. Jung, J. Kim and D. Kim, *Sens. Actuators, B*, 183 (2013) 381
25. F. Wolfart, A. L. Lorenzen, N. Nagata and M. Vidotti, *Sens. Actuators, B*, 186 (2013) 528
26. L. Yang, H. Xiong, X. Zhang, S. Wang and X. Zhang, *Biosens. Bioelectron*, 26 (2011) 3801
27. J. Y. Sun, K. J. Huang, Y. Fan, Z. W. Wu and D. D. Li, *Microchim. Acta*, 174 (2011) 289
28. T. R. Ling, C. S. Li, J. J. Jow and J. F. Lee, *Electrochim. Acta*, 56 (2011) 1043
29. R. Ojani, J. B. Raoof and P. Salmany-Afagh, *J. Electroanal. Chem*, 571 (2004) 571
30. A. Arvinte, A. M. Sesay and V. Virtanen, *Talanta*, 84 (2011) 180
31. R. P. Deo and J. Wang, *Electrochem. Commun*, 6, (2004) 284
32. S. Buratti, B. Brunetti and S. Mannino, *Talanta*, 76 (2008) 454
33. D. Salinas-Torres, F. Huerta, F. Montilla and E. Morallón, *Electrochim. Acta*, 56 (2011) 2464
34. K. E. Toghill, L. Xiao, M. A. Phillips and R. G. Compton, *Sens. Actuators B*, 147 (2010) 642
35. H. Nie, Z. Yao, X. Zhou, Z. Yang and S. Huang, *Biosens. Bioelectron*, 30 (2011) 28
36. A. J. Bard and L. R. Faulkner, *Electrochemical Methods: Fundamentals and Applications*, 2nd ed., John Wiley, New York (2001)
37. E. Laviron, *J. Electroanal. Chem*, 101 (1979) 19
38. G. Karim-Nezhad, M. Hasanzadeh, L. Saghatforoush, N. Shadjou, S. Earshad and B. Khalilzadeh, *J. Braz. Chem. Soc*, 20 (2009) 141
39. S. S. Kumar and S. S. Narayanan, *Electroanalysis*, 20 (2008) 1427

40. T. Bright and D. Y. Murzin, *Catal. Sci. Technol*, 3 (2013) 297
41. B.T. Kusema, B. C. Campo, P. Maki-Arvela, T. Salmi and D. Y. Murzin, *App. Catal. A*, 386 (2010) 101
42. D. Y. Murzin and T. Salmi, *Catal. Lett*, 142 (2012) 817
43. M. Rizzotto, M. I. Frascaroli, S. Signorella and L. F. Sala. *Polyhedro*, 9 (1996) 1517
44. L. Li, B. Liang, J. Shi, F. Li, M. Mascini and A. Liu, *Biosens. Bioelectron.*, 33 (2012) 100
45. P. Ruestschi, *J. Electrochem. Soc.* 106 (1959) 819
46. B. E. Conway, D. J. Mackinnon and B. V. Tilak, *Trans. Faraday soc*, 66 (1970) 1203
47. J. P. Brenet and K. Traore, *Transfer coefficients in Electrochemical kinetic*; Academic Press: London, (1971)
48. M. H. P. Santana, L. A. De Faria and J. F. C. Boodts, *Electrochim. Acta*, 50 (2005) 2017
49. M. H. P. Santana, L. A. De Faria and J. F. C. Boodts, *J. Appl. Electrochem*, 35 (2005) 915
50. H. J. Schafer and R. Scheider, *Tetrahedron*, 46 (1991) 715
51. A. Salimi, E. Sharifi, A. Noorbakhsh and S. Soltanian, *Biosens. Bioelectron*, 22 (2007) 3146
52. I. G. Casella, A. Destradis and E. Desimoni, *Analyst*, 121 (1996) 249
53. R. Holze, T. Luczak and M. Beltowska-Brzezinska, *Electrochim. Acta*, 39 (1994) 485

© 2014 The Authors. Published by ESG (www.electrochemsci.org). This article is an open access article distributed under the terms and conditions of the Creative Commons Attribution license (<http://creativecommons.org/licenses/by/4.0/>).